Published in final edited form as:
J Nucl Cardiol. 2010 April ; 17(2): 328–332. doi:10.1007/s12350-009-9145-2.

Cardiomyopathy of uncertain etiology: Complementary role of multimodality imaging with cardiac MRI and ^{18}FDG PET

Orla Buckley, MD[a], **Leona Doyle, MD**[b], **Robert Padera, MD**[b], **Neal Lakdawala, MD**[c], **Sharmila Dorbala, MD**[a,c], **Marcelo Di Carli, MD**[a,c], **Raymond Kwong, MD, MPH**[a,c], **Akshay Desai, MD**[c], and **Ron Blankstein, MD**[a,c]

[a]Noninvasive Cardiovascular Imaging Program, Departments of Radiology and Medicine (Cardiology), Brigham and Women's Hospital, Boston, MA

[b]Department of Pathology, Brigham and Women's Hospital, Boston, MA

[c]Cardiovascular Division (Department of Medicine), Brigham and Women's Hospital, Boston, MA

A 59-year-old female with longstanding history of tachyarrhythmias was admitted for syncope and recurrent ventricular tachycardia. She had a past medical history of hyperlipidemia, hypothyroidism, atrial fibrillation, and wide complex tachycardia that had been attributed to Wolf-Parkinson-White syndrome. Her medications included atenolol, propafenone, synthroid, and lipitor. Her 12-lead ECG was notable for sinus rhythm with marked 1st degree heart block, right bundle branch block, and left anterior fascicular block (Figure 1). The echocardiogram on admission demonstrated a moderately dilated left ventricle with normal wall thickness. There was global left ventricular hypokinesis with an estimated ejection fraction (LVEF) of 20%. There was mild right ventricular dilatation with mild global reduction in right ventricular systolic function.

To evaluate for possible obstructive CAD, the patient underwent invasive coronary angiography which demonstrated normal coronary artery anatomy with no evidence of atherosclerotic disease (Figure 2A, B).

An endomyocardial biopsy from the right ventricular septum was then obtained to evaluate for infiltrative disease. Five biopsy samples were acquired. The endomyocardial biopsy demonstrated diffuse subendocardial myocyte vacuolization, which was thought to be demand-related given the tachyarrhythmias and normal coronary arteries (Figure 3). Specifically, there was no evidence of active myocarditis, granulomatous inflammation, acute or recent myocardial infarction, amyloid heart disease, or iron deposition.

Cardiac Magnetic Resonance (CMR) imaging was performed to find a potential cause of her cardiomyopathy and source of her ventricular tachycardia. CMR demonstrated severe reduction in global systolic function with and LVEF of 24% and RVEF of 20%. There was no myocardial edema on T2 weighted sequences and no evidence of increased myocardial iron deposition. Delayed enhancement images acquired 10 minutes after injection of 0.15 mmol/kg gadolinium demonstrated abnormal enhancement of the thinned myocardium in a near transmural pattern, was most prominent along the basal to mid anterior wall and septum (Figure 4A, B, C). Collectively, the non-coronary distribution, the septal involvement, and

Reprint requests: Ron Blankstein, MD, Noninvasive Cardiovascular Imaging Program, Brigham and Women's Hospital, 75 Francis Street, ASB1-L1, Boston, MA 02115; rblankstein@partners.org.

the subendocardial sparing were features highly suggestive of a non-ischemic cardiomyopathy and raise the possibility for myocardial infiltration with sarcoid.

Given the incongruous results of the CMR and endomyocardial biopsy, there was a concern for a false negative biopsy. The patient subsequently underwent a rest ^{82}Rubidium and ^{18}FDG PET study, which demonstrated a medium sized perfusion defect with corresponding ^{18}FDG uptake (i.e., perfusion-metabolic mismatch) involving the mid and basal anterior and anteroseptal walls. In light of the fact that the patient had normal coronary arteries, this PET pattern was highly suspicious for an active inflammatory process (Figure 5). The whole body ^{18}FDG PET study also showed multiple ^{18}FDG avid lymph nodes in the cervical, mediastinal, and subdiaphragmatic regions (Figure 6).

Subsequent biopsy of a subcarinal lymph node demonstrated histological features of sarcoidosis (Figure 7). The patient was placed on immunosuppression and an implantable defibrillator was inserted.

Discussion

A minority of patients with systemic sarcoidosis have clinical symptoms of cardiac infiltration (5%) although up to half of autopsies performed on patients with systemic sarcoidosis show cardiac involvement.[1] Early diagnosis of cardiac infiltration is critical as a significant proportion of deaths in patients with systemic sarcoidosis can be attributed to arrhythmias secondary to cardiac infiltration and attendant scar formation.[1,2] Current diagnostic criteria are based on guidelines from Hiraga et al created in 1993.[3] These guidelines are based on histological demonstration of non-caseating granulomas on endomyocardial biopsy in the absence of any fungal or mycobacterial infection. Clinical components of the criteria include the presence of ECG abnormalities such as heart block or arrhythmias. Imaging criteria include the presence of a wall motion abnormality or reduced cardiac output on echocardiography, regional perfusion defect on thallium scintigraphy, abnormal accumulation of ^{67}Gallium or technetium pyrophosphate scintigraphy. These diagnostic criteria do not recognize the potential role of cardiac MRI or ^{18}FDG PET imaging in the diagnosis of cardiac infiltration by sarcoidosis.

In our case, the endomyocardial biopsy did not identify the diagnosis. Endomyocardial biopsy is a highly specific technique but with only 20–30% sensitivity.[4] This may be due to the fact that typically a right ventricular biopsy is obtained and most commonly of the right ventricular apical septum. Sarcoidosis, however, often involves the basal to mid septum but can involve the left ventricular myocardium also. These areas would not be sampled in the typical areas biopsied.

Role of cardiac MRI

The contribution of CMR for tissue characterization in the assessment of cardiomyopathy and specifically in the evaluation of patients with suspected or known sarcoidosis is now well recognized. Patel et al in a study of 58 patients showed that CMR detected cardiac involvement in twice as many patients than ECG or echocardiography.[5] CMR may detect disease earlier than the conventional diagnostic approaches,[6] and has the possible advantage of directing biopsy to focal areas of infiltration. However, the correlation between degree of myocardial scarring and risk of ventricular arrhythmia has not been clearly defined.

In our case, CMR demonstrated several features suggestive of the post inflammatory pattern of sarcoidosis including wall thinning and delayed enhancement in a non-coronary artery distribution which spared the subendocardium. [7] The absence of edema on T2 weighted sequences suggested that this was not an acute inflammatory process. While CMR features

of sarcoid typically demonstrates nodular T2 weighted hyper intensities, in our case, such focal nodular hyper intensities were not present. The diffuse distribution of late enhancement in our case is not typical for sarcoid.

Role of ^{18}FDG PET

Traditional nuclear medicine techniques used to evaluate for cardiac involvement in with sarcoidosis include ^{201}Thallium or ^{99m}Tc-labeled tracers and SPECT. However, a regional perfusion defect is not specific and can be seen in ischemic cardiomyopathy. Although included in the diagnostic criteria for cardiac involvement with sarcoidosis,[8] ^{67}Ga scintigraphy has low sensitivity and specificity for the detection of cardiac sarcoidosis.

Fasting ^{18}FDG PET has been shown to be a useful technique in the diagnosis of cardiac sarcoidosis.[8] One of the challenges with this approach is that normal myocardium can take up ^{18}FDG even under fasting conditions. Thus, the success of this approach hinges upon the successful suppression of ^{18}FDG uptake in normal myocardium and requires careful patient preparation. At our institution, patients are asked to ingest a high fat, low carbohydrate, high protein diet the day before the scan. The patient then fasts for at least six hours prior to the scan. The patient is instructed to specifically avoid sugar and sugar containing foods. The purpose of this protocol is to shift normal myocardial metabolism to fatty acid oxidation. The scan sequence includes a resting myocardial perfusion study first with ^{82}Rubidium. After perfusion imaging, ^{18}FDG is injected and images are acquired approximately 90 minutes following radiotracer injection. The increased ^{18}FDG PET uptake in cardiac sarcoidosis is thought to be due to accumulation of macrophages and reactive lymphocytes in the inflammatory tissue.

This is an evolving application for PET imaging and the range of patterns of ^{18}FDG uptake in cardiac sarcoidosis are being evaluated. It is possible that in early stages of inflammation may be associated with increased myocardial ^{18}FDG uptake in the absence of regional perfusion defects. As disease progresses, regional perfusion defects are likely to result from microvascular compression caused by accumulation of inflammatory cells and edema, and/or replacement fibrosis. In active sarcoidosis, these areas of resting perfusion deficit show increased metabolic activity and have the appearance of the classic perfusion-metabolic mismatch pattern, as in our case. Because regional perfusion defects with or without concomitant metabolic activity can also results from ischemia/infarction, PET findings must be interpreted in the context of coronary angiographic findings. The concomitant evaluation of extracardiac uptake of ^{18}FDG is helpful in increasing diagnostic certainty. In our case, multiple foci of ^{18}FDG avid lymph nodes were identified in the mediastinum and chest. This in turn can help guide biopsy of extracardiac lymph nodes as was the case in our patient.

Complementary roles of ^{18}FDG PET and CMRI

Using current diagnostic criteria the diagnosis of sarcoidosis would have been missed. In the management of this patient, CMR and ^{18}FDG PET demonstrated their inherent individual and complementary strengths: the anatomic diagnosis permitted by CMR and the ability of ^{18}FDG PET to demonstrate inflammatory activity in the myocardium and serve as a marker to monitor therapeutic response.[9]

References

1. Matsui Y, Iwai K, Tachibana T, et al. Clinicopathological study of fatal myocardial sarcoidosis. Ann N Y Acad Sci. 1976; 278:455–469. [PubMed: 1067031]
2. Tachibana, T.; Iwai, K.; Takemura, T. Study on the cause of death in patients with sarcoidosis in Japan; Presented at XII World Congress on Sarcoidosis, Kyoto, Japan; 1991.

3. Hiraga, H.; Yuwai, K.; Hiroe, M., et al. Guideline for the diagnosis of cardiac sarcoidosis study report on diffuse pulmonary diseases. Tokyo: Japanese Military of Health and Welfare; 1993. p. 23-24.

4. Sekiguchi M, Yazaki Y, Isobe M, et al. Cardiac Sarcoidosis: Diagnostic, prognostic and therapeutic considerations. Cardiovasc Drugs Ther. 1996; 10:495–510. [PubMed: 8950063]

5. Patel MR, Cawley PJ, Heitner JF, et al. Delayed enhanced MRI improves the ability to detect involvement in patients with sarcoidosis. Circulation. 2004; 110:2995.

6. Smedema JP, Snoep G, van Kroonenburgh MPG, van Geuns RJ, et al. The additional value of enhanced MRI to standard assessment for cardiac involvement in patients with pulmonary sarcoidosis. Chest. 2005; 128:1629–1637. [PubMed: 16162768]

7. Vignaux O. Cardiac sarcoidosis: Spectrum of MRI features. AJR. 2005; 184:249–254. [PubMed: 15615984]

8. Yamagashi H, Shirai N, Takagi M, et al. Identification of cardiac sarcoidosis with ^{13}N-NH3/^{18}FDG PET. J Nucl Med. 2003; 44:1030–1036. [PubMed: 12843216]

9. Okumuro W, Iwasaki T, Toyama T, Iso T, Arai M, Oriuchi N, et al. Usefulness of fasting PET in the diagnosis of cardiac sarcoidosis. J Nucl Med. 2004; 45(12):1989–1998. [PubMed: 15585472]

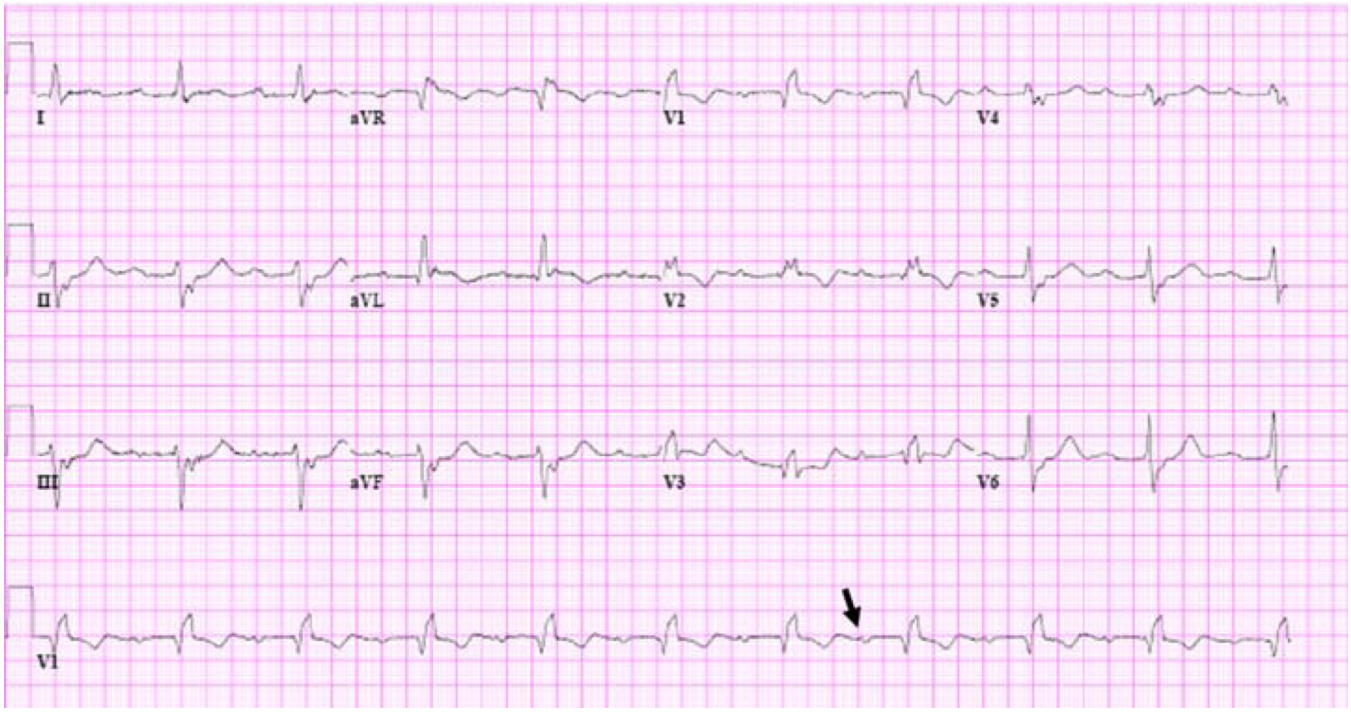

Figure 1.
12 lead ECG notable for Sinus rhythm (*black arrow* indicates p wave) with marked 1st degree heart block, right bundle branch block and left anterior fascicular block.

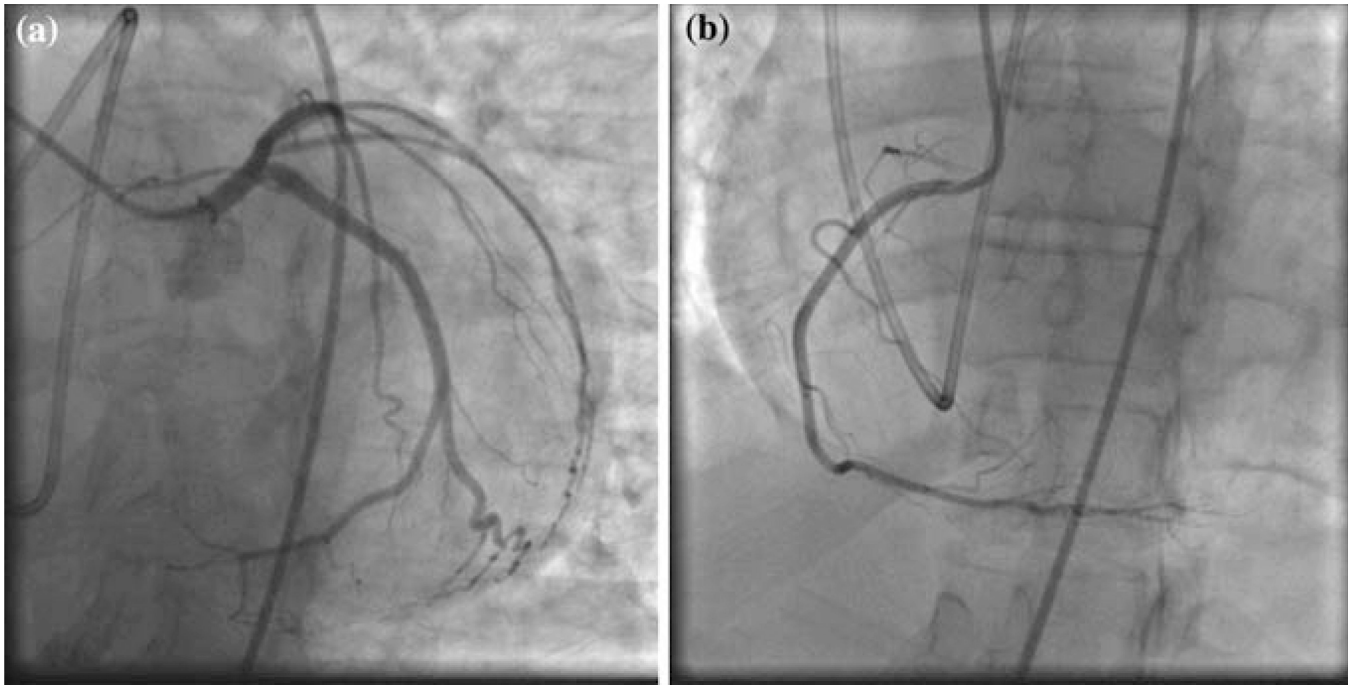

Figure 2.
Coronary angiography found no evidence of coronary artery disease, **A** shows the selective catheterization and opacification of the LAD and LCX, and **B** the RCA.

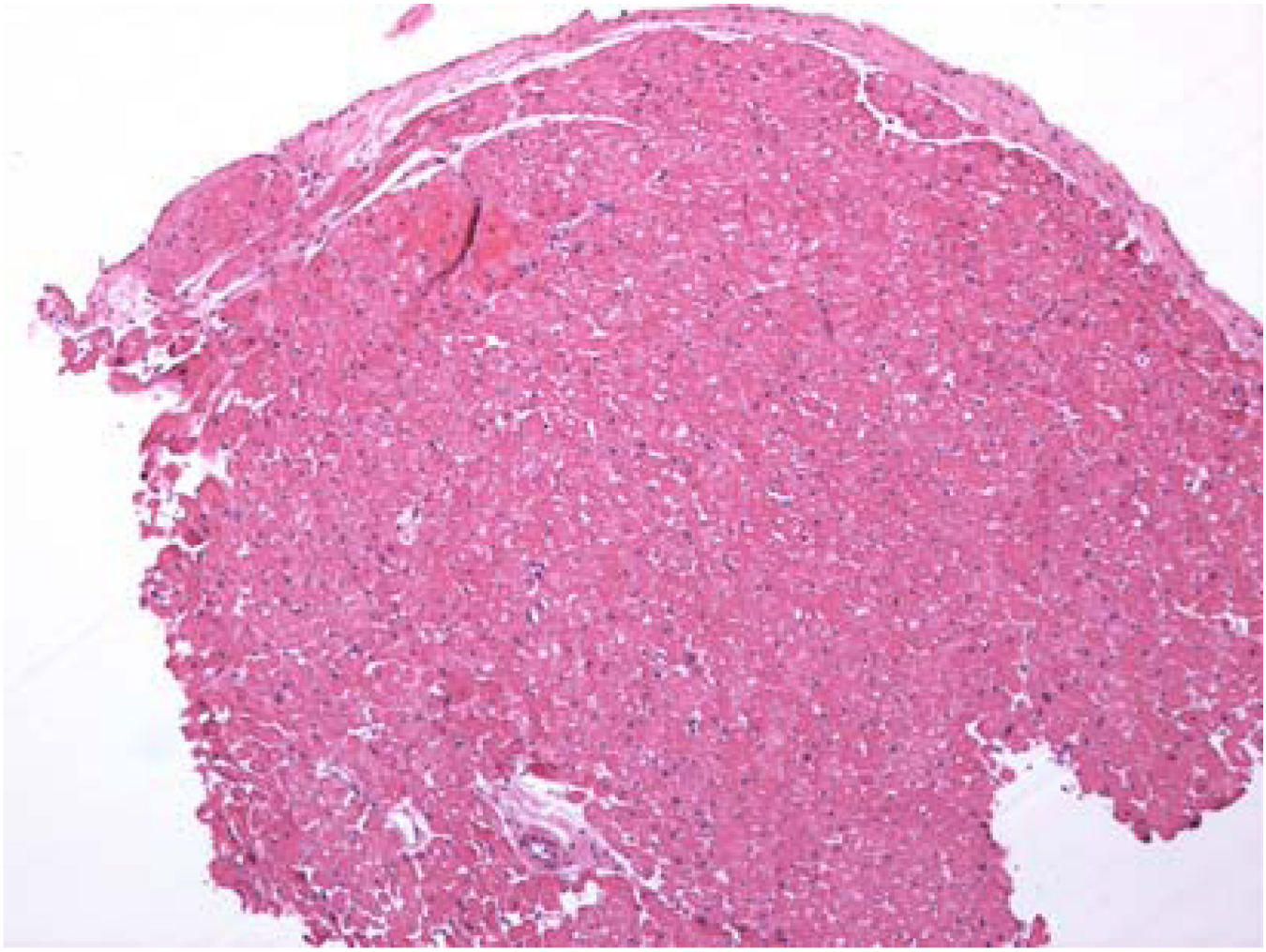

Figure 3.
Endomyocardial biopsy shows no evidence of granulomatous disease. There is diffuse subendocardial myocyte vacuolization suggestive of chronic ischemia thought to be related to demand-related given the tachyarrhythmias and normal coronary arteries.

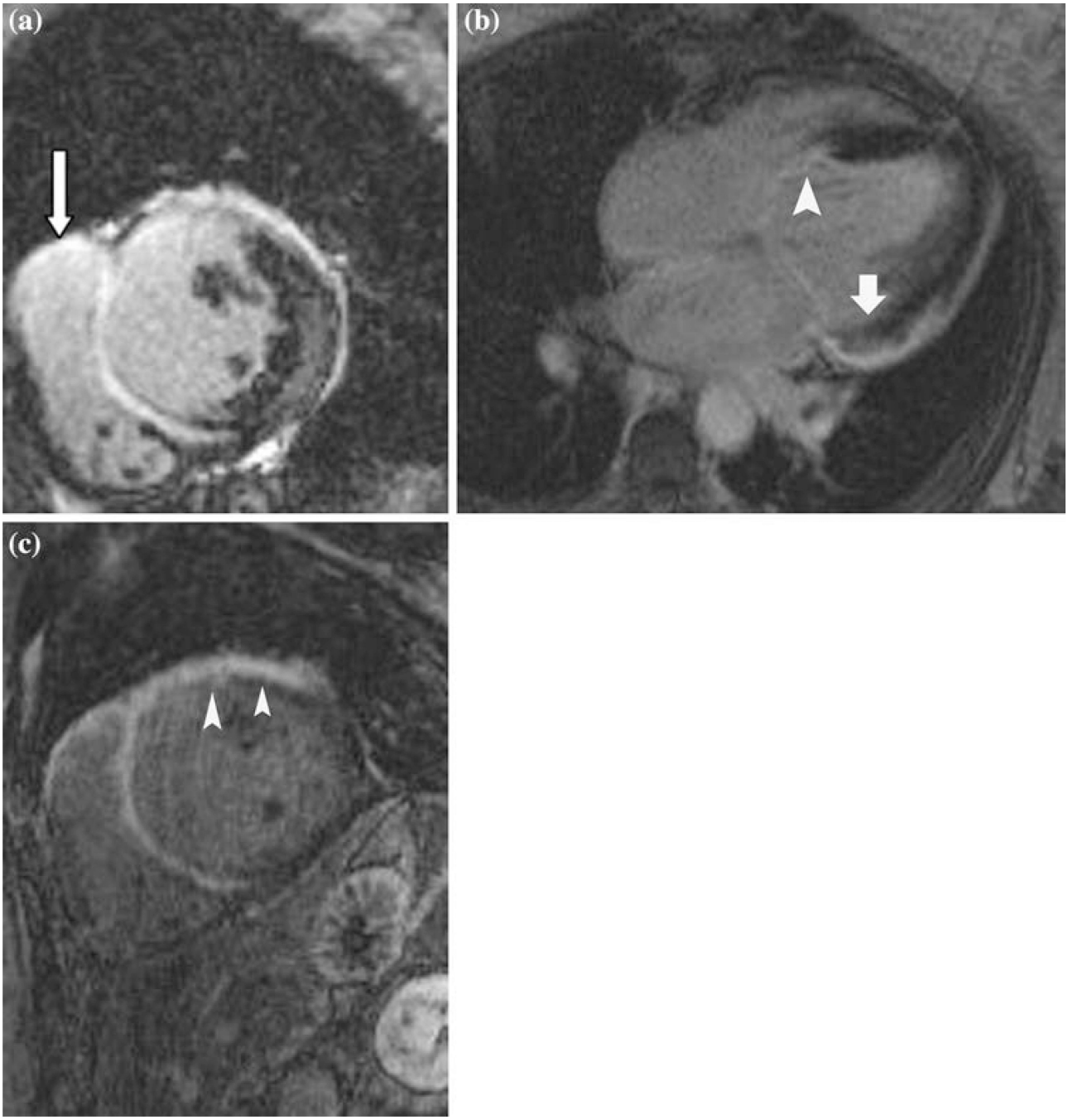

Figure 4.

A Myocardial late gadolinium enhanced imaging of the short axis of the basal myocardium shows myocardium thinning and diffuse transmural late gadolinium enhancement which spares only the inferior and inferolateral segments. Late gadolinium enhancement is also seen in the anterior right ventricular wall (*arrow*). **B** Four chamber image shows near transmural late gadolinium enhancement of the basal septum (*white arrowhead*) and non-transmural subepicardial enhancement of the basal to mid lateral wall (*white arrow*). **C** High resolution free breathing navigator guided sequence shows the late gadolinium enhancement of the basal myocardium spares the endocardium (*arrowheads*).

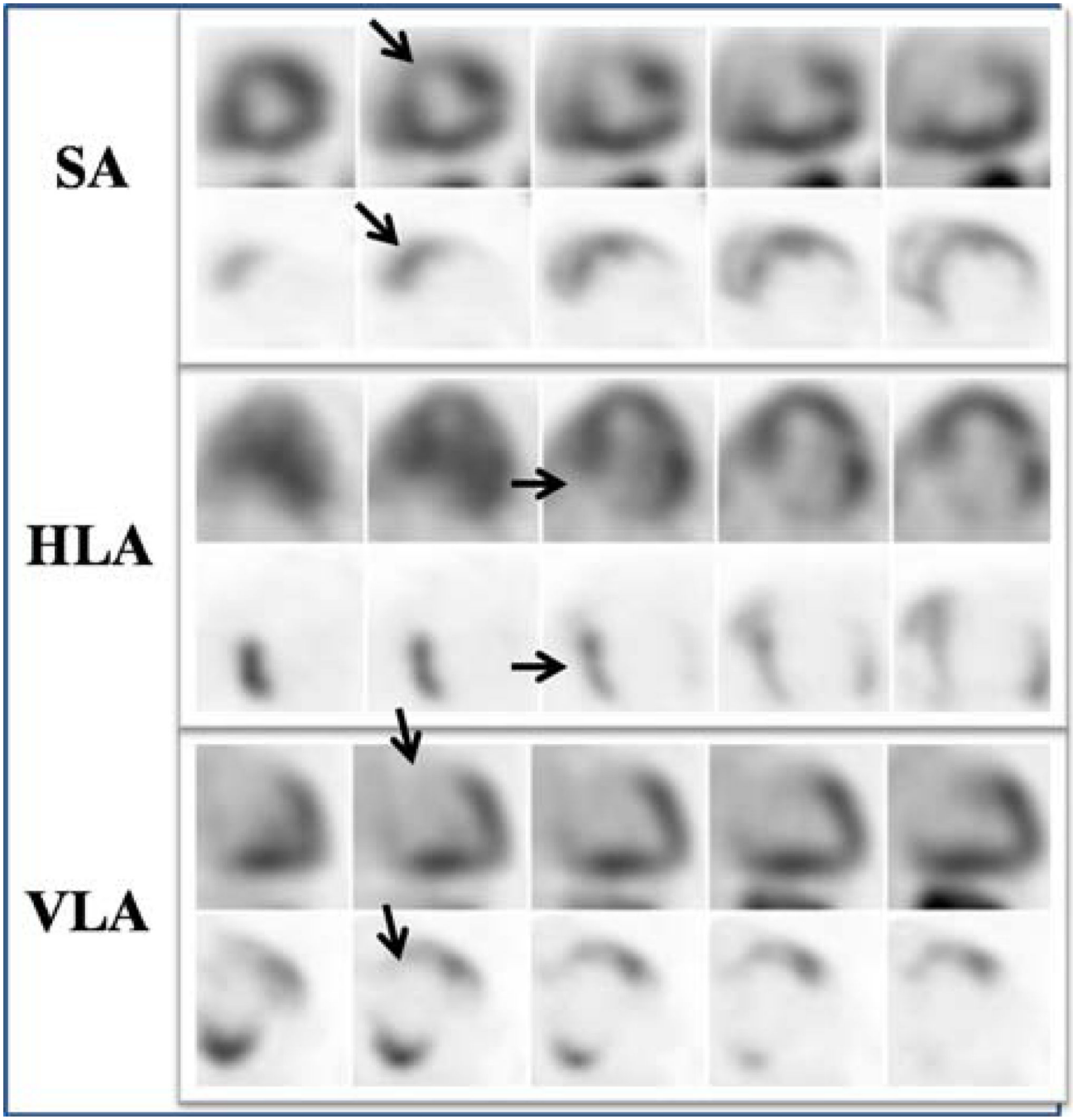

Figure 5.
Resting ^{82}Rubidium PET myocardial perfusion images showing a perfusion abnormality in the basal to mid anterior and antero septal segments (*top row*). This defect is matched on ^{18}FDG PET images by focal ^{18}FDG PET avidity in the basal to mid anterior and antero septum (*bottom row*).

Figure 6.
Coronal image from the ^{18}FDG PET study demonstrates ^{18}FDG avid left supra clavicular node and mediastinal nodes (*white arrows*) and myocardium.

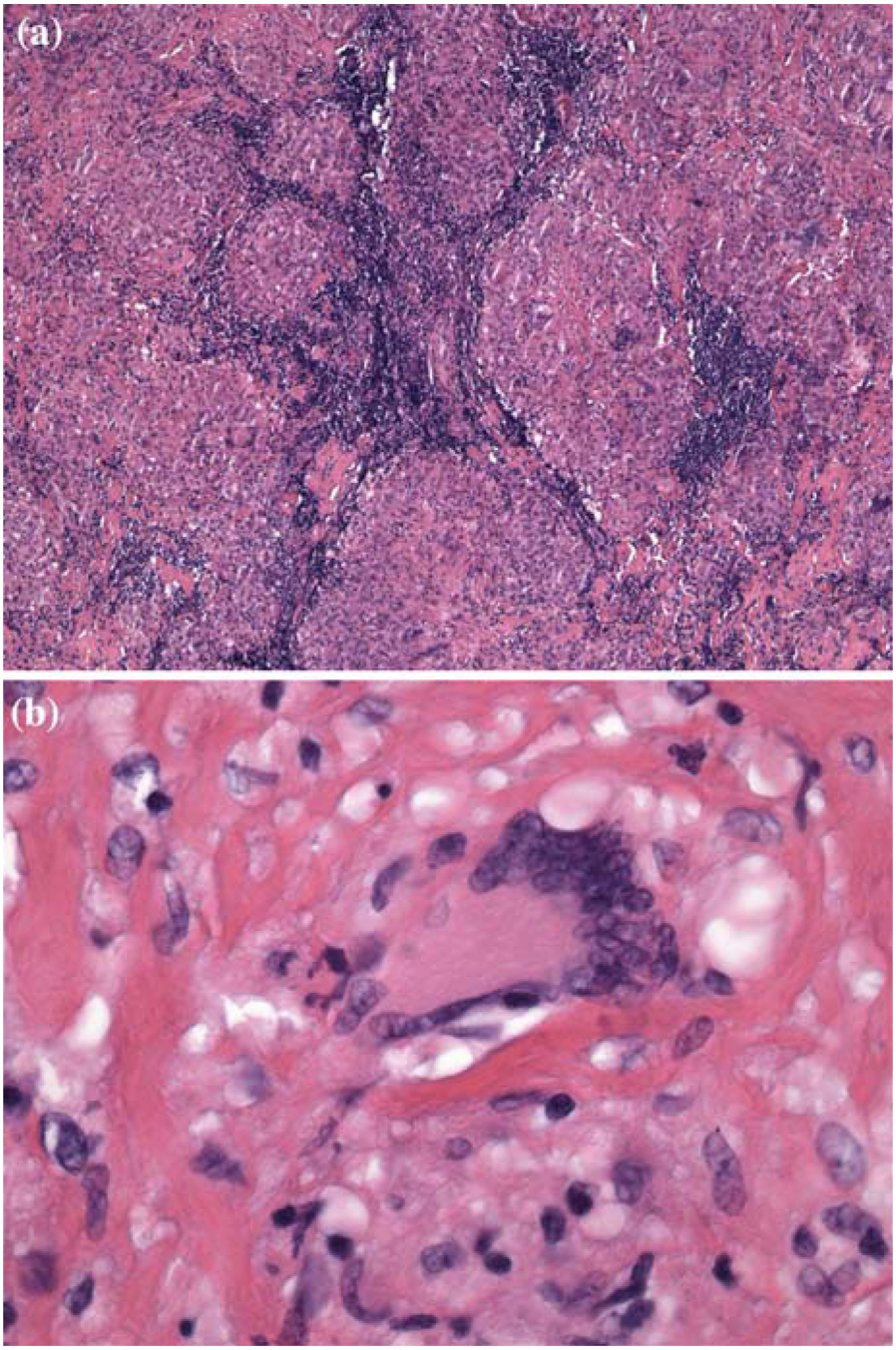

Figure 7.

A and **B** is a low power image of the lymph node biopsy from a subcarinal lymph node which shows effacement of normal lymph node architecture by well-formed non-necrotizing granulomata. Higher power image in **B** demonstrates a high power image of the granulomatous inflammation demonstrating a giant cell surrounded by epithelioid histiocytes. The histological features were consistent with the diagnosis of sarcoidosis.